Noise spectroscopy data analysis-based gas identification with a single MOX sensor

Nicolas Morati, Thierry Contaret, Sami Gomri, Tomas Fiorido, Jean-Luc Seguin, Marc Bendahan

Noise spectroscopy data analysis-based gas identification with a single MOX sensor

Nicolas Morati[1], Thierry Contaret[1,*], Sami Gomri[2], Tomas Fiorido[1], Jean-Luc Seguin[1] and Marc Bendahan[1]

[1]*Aix Marseille Univ, Université de Toulon, CNRS, IM2NP, Marseille, France*
[2]*METS Unit, National School of Engineers of Sfax, Sfax, 3038, Tunisia*

*Corresponding author: thierry.contaret@im2np.fr

Keywords: MOX gas sensor; noise spectroscopy; multivariate analysis; gas discrimination

Abstract

Air quality monitoring and analysis have become a major issue in recent years. Metal oxide (MOX) gas sensors are very sensitive due to high variability of their resistivity in presence of gas. However, they are not selective, i.e. it is not possible to determine the nature and concentration of the gas using only variations in the resistance of the sensor. Noise spectroscopy is one of the solutions to improve selectivity. In this paper, we evaluate recent noise spectroscopy-based gases identifications methods, to distinguish the nature of different gases using a single MOX sensor. From noise measurements performed on MOX gas sensors with tungsten trioxide (WO_3) sensing layer, under several nitrogen dioxide (NO_2), ozone (O_3) and carbon monoxide (CO) concentrations in dry air, we have created a database. This database is increased by extracting the spectral attributes of noise responses, and then reduced by using principal component analysis to extract only useful information. The results

obtained in this study demonstrated that it is possible to distinguish three air quality gases with only one single WO_3 sensor.

1. Introduction

Nowadays, there is a growing need for low-cost, low-power, miniaturized gas sensors mainly due to the connectivity of sensing devices on global network (internet of things) enabling immediate sharing of information in a variety of fields such as portable and connected devices for domestic and industrial air quality control, security and defence, food quality control …

In the case of air quality where health, social and political issues have become important to the population, there is a strong demand for air pollution monitoring systems. Indeed, air pollution is characterized by the presence of a set of important pollutants of chemical origin (VOC, fine particles, ozone, nitrogen dioxide, carbon monoxide and sulphur dioxide) and biological (molds, mites). As this variety of pollutants is large and the concentrations harmful to health are very low and permanent in ambient air, it has become imperative to design detection systems that are sufficiently sensitive to detect and discriminate between several gases in polluted ambient air. In this context, a great deal of research and development work is being carried out to design small and cheap gas sensors with high sensitivity, selectivity and stability, with respect to a given application. Metal oxide (MOX) gas sensors are readily available and widely used in portable and low cost gas monitoring devices because of their high sensitivity, stability, and attractive life time. However, this type of gas sensor suffers an inherent lack of selectivity, because the gas detection mechanism is rather unspecific and more or less any type of reducing or oxidizing gas is detected.

Due to this poor selectivity, MOX gas sensors are more often assembled into a multi sensor array that forms the core of an electronic nose. Electronic nose is a complex system used in

the identification of gas mixtures. It consists of a multi sensor array, an information-processing unit, software with digital pattern-recognition algorithms and reference-library databases [1-2]. The sensor array is composed of different sensors chosen to respond to a wide range of chemical classes. The outputs of individual sensors are collectively assembled and integrated to generate a distinct digital response pattern. Identification and classification of an analyte mixture is accomplished through recognition of this unique chemical signature (electronic fingerprint) of collective sensor responses. The challenge in miniaturizing devices and lowering power consumption is to minimize the number of sensors required for a given application. To do this, we must try to increase the amount of information provided by one sensor using advanced measurements, like temperature modulation or fluctuation enhanced sensing (FES). [3, 4].

The FES principle uses the fluctuations of the gas sensors' response as an information source. This experimental technique is based on noise spectroscopy: the measurement and the analysis of the power spectral density (PSD) of the fluctuations measured at the terminals of sensors in the presence of one or more gases. Measuring these fluctuations caused by adsorption–desorption and diffusion noise provides enhanced selectivity and sensitivity. Several studies have shown that noise spectroscopy is a relevant signal-processing tool able to extract selective informations on multiple gases with a single sensor [4-6].

In earlier work [26], we developed a model of adsorption–desorption (A-D) noise based on the physical origin of noise in MOX sensors. From this model, we developed three gases identifications methods able to discriminate several gases characterizing air quality, as well as their concentration, with a single MOX sensor, under real operating conditions, i.e. in the permanent presence of a gas concentration.

The capability of discriminating gases was evaluated using Principal Component Analysis (PCA). The content is organized as follows:

(i) Section 2: General methodology

(ii) Section 3: Measurement methods and device

(iii) Section 4: Noise spectroscopy-based gases identifications methods

(iv) Section 5: Results

(v) Section 6: Conclusion

2. General methodology

Enhancement of the MOX gas sensors selectivity has been the subject of many studies for decades. Different measurement methodologies (dynamic response by thermal modulation, response in pulsed thermal mode, sensors arrays, noise spectroscopy…) associated with signal processing algorithms (Fast Fourier Transform, PCA, neural networks…) have been developed and have shown their possibilities [8-11]. The gas detection and identification technique that we are developing is focused on low frequency noise spectroscopy.

The interest of measuring the noise response of a gas sensor comes from observing the change in spectral density of fluctuations in the resistance of the sensor in the presence of several gases. The advantage of this measurement technique is to acquire the response of the sensor in steady mode, ie after the response time of sensor. Furthermore, this technique does not depend on the characteristics of the dilution system of an experimental measurement bench and makes it possible to approach detection in the permanent presence of a gas mixture. The statistical study of microscopic fluctuations generating sensor resistance fluctuations constitutes an important source of information on the sensor itself. This high sensitivity is based on the fact that disturbances of microscopic fluctuations require only very low energy.

The statistical distribution functions characterizing these fluctuations are data tables, which can contain a quantity of information greater by several orders of magnitude than that provided by a simple quantity, such as the variation of the resistance of the sensor used in classical measurement. In addition, the noise parameters that can be extracted from noise responses have a physical origin in the adsorption-desorption process of the gas molecules on the surface of the sensitive layer of the sensor.

Used methodology for our study is summarized in Fig. 1. First, a noise response database is created by measuring the power spectrum of the amplified current fluctuations across the sensor when the concentration of the target gas is constant. The noise measurement system for gas sensors is described in section 3. Then, the database is increased by extracting the spectral attributes of the noise responses using the characterization methods presented in section 4, and then reduced using principal component analysis to extract only useful information. Gas discrimination is achieved by the online projection of measurements in the principal space consisting of the two main components. PCA is a robust and unsupervised model recognition approach commonly used for multivariate data analysis. It is a statistical procedure that converts a set of observations of possibly correlated variables into a new set of values called principal components. PCA has proven its effectiveness in many areas of application [12-14], including electronic noses [15]

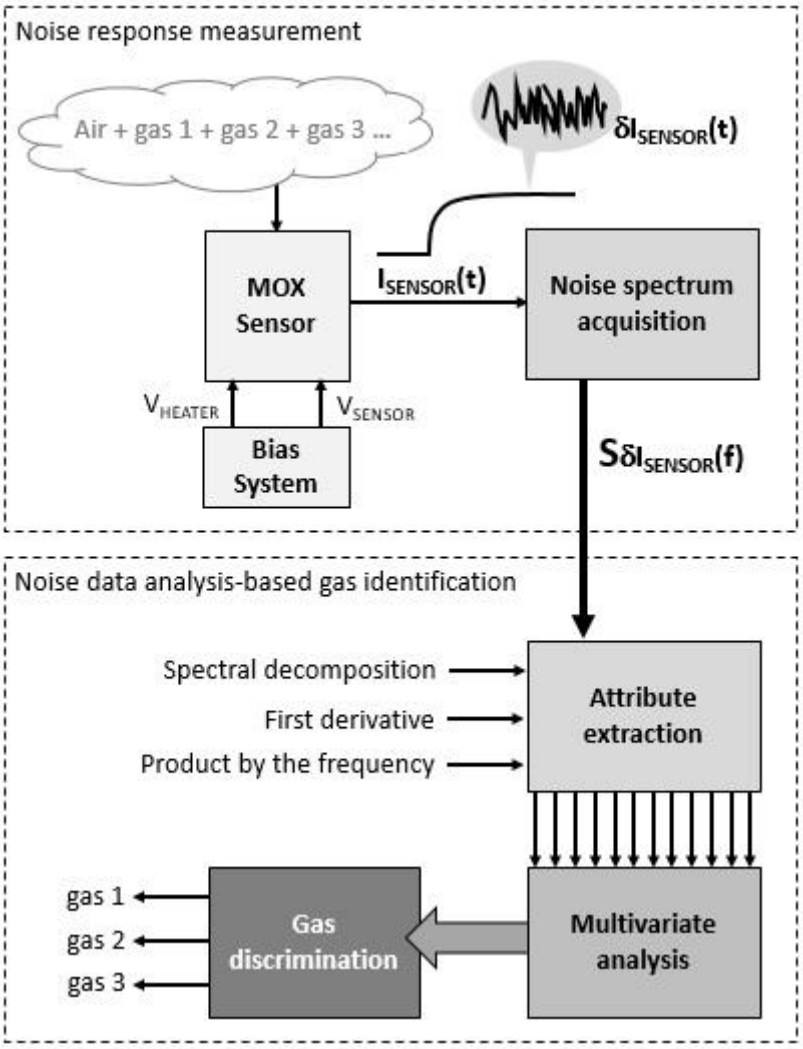

Fig. 1. Summary of the methodology used

3. Measurement methods and device

The specific noise spectroscopy system to measure the sensor noise response in air, nitrogen dioxide, carbon monoxide and ozone is the same one used in our recent paper [16]. It is presented in Fig.2. The power spectrum of the amplified current fluctuations across the sensor is measured using low noise current preamplifier and FFT spectrum analyser. The sensors are placed in a stainless steel measurement chamber where mixed gases can be admitted and evacuated via distribution valves. To obtain a linear flow and homogeneous mixture, the incoming gases are mixed by a diffuser after electronic gas flow controllers. The gas chamber,

the preamplifier, the sensors biasing and the power supply for sensor local heating are incorporated in a Faraday cage.

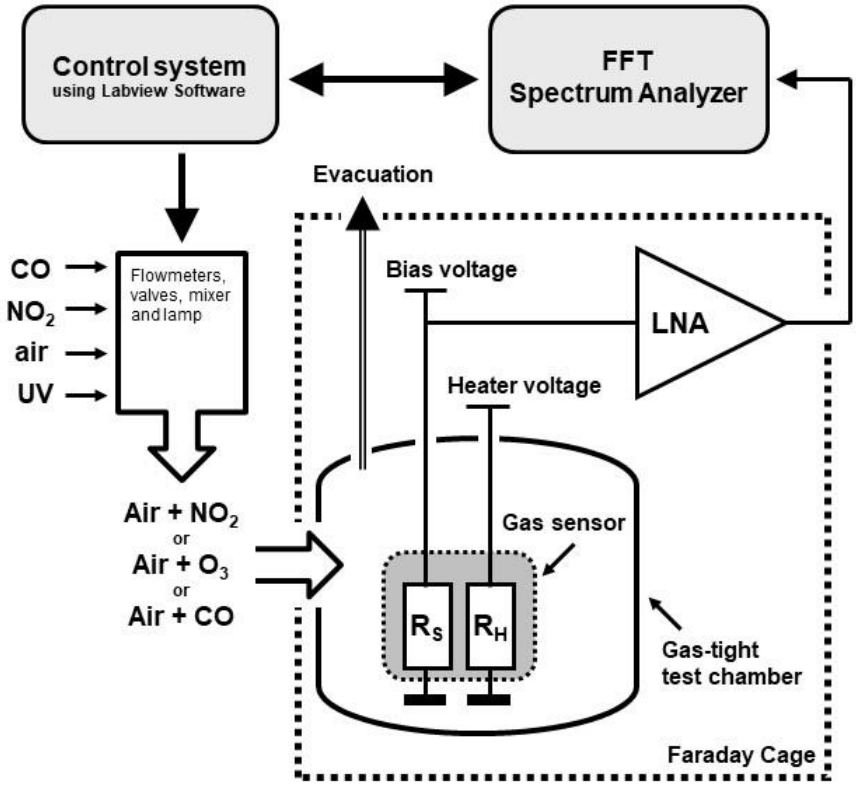

Fig. 2. General diagram of measurements setup used to characterize microsensors noise responses.

The studied MOX gas sensors are based on tungsten trioxide (WO3). WO3 thin films were prepared by reactive radio frequency (13.56 Mhz) magnetron sputtering, using a 99.9% pure tungsten target. The thickness of the WO_3 film is about 40 nm. The films were sputtered on SiO_2/Si substrates with platinum interdigitated electrodes, in a reactive atmosphere of oxygen-argon mixture. The microsensor doesn't have an integrated heating device. It was placed on a heated plate and biased by a voltage of 1V with a specific system of microtips. For more details concerning the preparation of the WO_3 based sensing layer, one can see the descriptions given in [16]. As the resistance of the sensing layer is very high (MΩ range), and for best measurement conditions, the sensor is biased by a voltage source, and the fluctuation

of the current crossing the sensing layer is amplified by a low noise current amplifier Stanford Research SR570 (LNA on figure 1). The power spectrum density (PSD) of the outputted voltage is recorded using a SR785 FFT Signal Analyzer, in the 0.1Hz-100kHz range, at a sampling rate of 256 000 samples/s. The build in high pass filter of the SR570 amplifier was set to a cutoff frequency of 0.03Hz with a -12dB/octave slope. The PSD of the current fluctuations was recorded when the gas microsensor was exposed to the target gas diluted in dry air and the sensor resistance was constant (steady state operating). The measurement time is about 10 mn, mostly depending on the number of measurement points in the lowest frequency decades.

The gas microsensor was exposed to 4 concentrations of three different gases characteristic of the air quality (see Table I), diluted in dry air. These are ozone and nitrogen dioxide, which are oxidizing gases, and carbon monoxide, which is a reducing gas. For each gas, the acquisition of the noise spectrum begins when the response of the sensor is stable (steady regime). Figure 3 shows an example of sensor response for an ozone concentration of 80 ppb for the complete measurement duration.

TABLE I. VARIOUS GASES CONCENTRATION USED IN EXPERIMENTAL SET UP

Gases	Concentrations			
	C1	C2	C3	C4
NO_2	1 ppm	2 ppm	5 ppm	10 ppm
O_3	80 ppb	110 ppb	160 ppb	240 ppb
CO	5 ppm	10 ppm	20 ppm	40 ppm

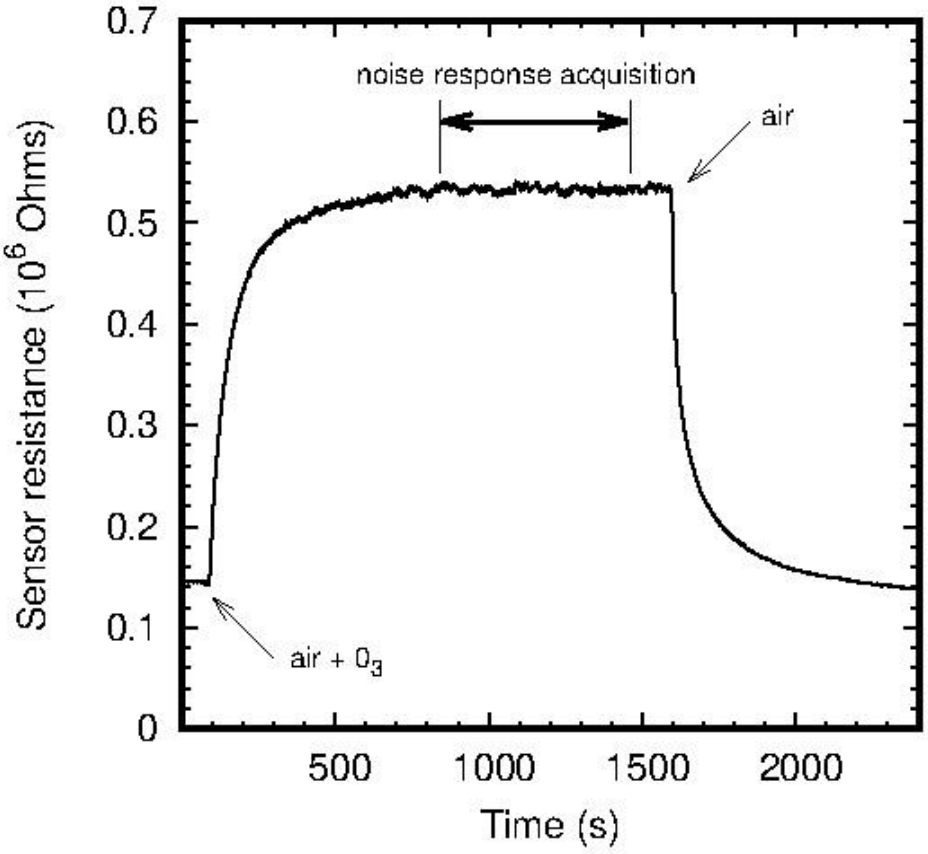

Fig. 3. Example of a response of studied WO_3 gas sensor under 80ppb ozone (O_3) concentration.

4. Noise Spectroscopy-based Gases Identifications Methods

In this section, we first present the main noise sources present in MOX sensors. Then, we briefly describe the noise spectroscopy-based gases identifications methods developed in previous work.

4.1 Noise sources in MOX gas sensors

In MOX gas sensors, we observe intrinsic noise sources similar to those found in semiconductors, and additional noise sources related to the chemical processes on the surface of the sensitive layer. Intrinsic noise sources are:

(i) The shot noise due to fluctuations of the carriers that create the conduction current. At low frequencies, the spectral density of conduction current is constant and is written:

$$S_{I_{cond}} = 2 \cdot q \cdot I_{cond} \tag{1}$$

where I_{cond} is the conduction current;

(ii) Thermal noise due to thermal agitation of the charge carriers in the semiconductor which causes voltage fluctuations. The noise current spectral density related to these voltage fluctuations is written:

$$S_{I_{th}} = 4 \cdot k \cdot T \cdot G \tag{2}$$

where k is the Boltzmann constant, T is the thermodynamic temperature and G is the conductance of semiconductor. The thermal noise is thus a white noise;

(iii) The generation-recombination (G-R) noise caused by the carriers' number fluctuations associated with the processes of generation and recombination. It's an excess noise in addition to fundamental noise sources (shot noise and thermal noise). The spectral density of current fluctuations associated with the capture and emission of carriers by a single trap in the bulk semiconductor is given by the relation:

$$S_{I_{G-R}} = \frac{K_{LF}}{1 + 4\pi^2 f^2 \tau^2} \tag{3}$$

where K_{LF} is the current noise spectral density at low frequencies proportional to the G-R induced variation on the current, and τ the average time associated with a trap. When the generation-recombination involves interface traps, the phenomenon is called Random Telegraph Signal (RTS). If the fluctuations come from a large number of generation-recombination process, the spectral density approximately varies as 1/f in the low frequencies band [17]. The 1/f noise or flicker noise is predominant over the thermal noise or shot noise. It involves various energy traps. It is located in the bulk [18] or at the surface of semiconductor, or at the interface between semiconductor and electrical contact [19]. It is known that the characterization of excess noise in microelectronics devices is a measure of performance and quality. It provides relevant information on the traps density, type and location [20].

The additional noise sources in the metal-oxide gas sensors are related to the properties of the metal-oxide sensitive layer and the chemical environment. In metal oxides, the noise depends strongly on the oxygen stoichiometry and displacement of oxygen atoms. The electronic charge transport is associated with the presence of oxygen at the surface and in the crystal lattice sites of the metal-oxide. The adsorption-desorption process of oxygen atoms and the presence of inhomogeneities, stresses and grain boundaries in the metal oxide cause fluctuations of the oxygen density and, thus fluctuations of the electrical conductance [21].

In a gaseous environment, conductance fluctuations of microsensors due to free carrier's number and mobility fluctuations are thus related to concentration and distribution

fluctuations of chemical species. The measured noise spectra result from the superposition of three noise sources contributions:

(i) The adsorption-desorption (A-D) noise due to the adsorption-desorption of gas molecules. It is similar to the G-R noise in intrinsic semiconductor;

(ii) The diffusion noise related to the diffusion of molecules adsorbed on the surface;

(iii) The shot noise due to the current through the potential barriers at grain boundaries in the sensitive layer.

The dominant noise source in gas microsensors is the adsorption-desorption noise [22]. The modelling of the spectral behavior of A-D noise source is based on Wolkenstein's theory [23]. Electrical conductivity fluctuations due to free carrier number and mobility fluctuations are proportional to the density fluctuations of adsorbed molecules:

$$S_{\delta\sigma}(f) = \sigma_0^2 \; S_{\delta N}(f) \tag{4}$$

where $S_{\delta\sigma}(f)$ is the power spectral density (PSD) of electrical conductivity fluctuations. σ_0 depends on free carrier density and mobility at adsorption-desorption equilibrium. $S_{\delta N}(f)$ is the PDS of adsorbed molecules density fluctuation which can be written [24,25]:

$$S_{\delta N}(f) = H_0 \; \frac{1}{1+\left(\frac{f}{f_c}\right)^2} \tag{5}$$

where

$$\begin{cases} H_0 = 4\ \overline{\delta N^2}\ \tau \\ f_c = \dfrac{1}{2\pi\tau} \end{cases} \tag{6}$$

$\overline{\delta N^2}$ is the mean square value of the adsorbed molecules density fluctuation δN. The time constant τ is

$$\tau = \left[\left(\frac{\mathrm{d}d}{\mathrm{d}N} \right)_{eq} - \left(\frac{\mathrm{d}a}{\mathrm{d}N} \right)_{eq} \right]^{-1} \tag{7}$$

where a and d are the number of adsorbed and desorbed molecules per unit area, respectively. Whether using Langmuir's theory or Wolkenstein's theory, calculating the time constant shows dependence with the gas parameters (mass of adsorbed molecule, adsorption energy, gas partial pressure …). So, H_0 and f_c are function of gas species. Details of the calculation of τ and $\overline{\delta N^2}$ can be found in Reference [15].

In earlier work [26], we presented a model of adsorption–desorption (A-D) noise in MOX gas sensors, developing the idea that the fluctuation of the gas sensor resistance is, among other noise sources, due to the fluctuation of the density of gas molecules on the surface of the sensing film. The modeling was developed by taking into account the polycrystalline structure of the sensing layer and the effect of the adsorbed molecule's density fluctuation on the grain boundary barrier height. From this model based on the physical origin of noise in MOX sensors, we developed three gases identifications methods. The first is based on the spectral decomposition of the noise responses. The second method uses the calculation of the first

derivative of noise current spectral density, and the third, the product of the noise current spectral density by the frequency.

4.2 Noise current spectral decomposition

As the dominant noise source in gas sensors is A-D noise, low frequency noise spectra are characterized by a sum of several Lorentzian. The power density spectrum (PDS) of fluctuations of the total sensing layer resistance $\delta Rsensor$ is written [25]:

$$S_{\delta Rsensor}(f) = \sum_{i=1}^{g} S_i \frac{1}{1+\left(\frac{f}{f_{ci}}\right)^2} \tag{8}$$

where g is the number of most prevalent grain sizes involved in the sensing layer. S_i and f_{ci} are, respectively, the low frequency noise level and the cut-off frequency of the Lorentzian number i. Their expressions are given in [25] and they depend on the nature of the detected gas, and on the grain size. If the gas sensor resistance R_{sensor} is biased by a voltage V_0, the measured noise is converted into a current noise. It thus takes into account the contribution of A-D noise generated in the gas sensor resistance and converted into a current noise, and the contribution of thermal noise generated by the sensing layer resistance. The PSD of the fluctuations of the total terminal current across the gas sensor resistance can be written [25]:

$$S_{\delta I_{sensor}}(f) = \frac{V_0^2}{R_{sensor}^4} \sum_{i=1}^{g} S_i \frac{1}{1+\left(\frac{f}{f_{ci}}\right)^2} + \frac{4kT}{R_{sensor}} \tag{9}$$

At low frequencies the A-D noise will dominate and at high frequencies its will be dominated by a white noise due to the thermal noise induced by the sensing layer resistance. As the

Lorenzian parameters depend on the nature and the concentration of the gas, the spectral decomposition of each spectrum enables to extract the noise parameters for each gas.

4.3 First derivative of noise current spectral density

In our recent work [26], we calculated the theoretical expression of the first derivative of the PSD of the gas sensor noise, and showed that it admitted a minimum which depends on the nature of the detected gas.

Using "(9)", the expression of the first derivative of the PSD of the gas sensor noise can be written as follows:

$$\frac{dS_{\delta I_{sensor}}(f)}{df} = -2\frac{V_0^2}{R_{sensor}^4}\sum_{i=1}^{g}\frac{S_i}{f_{ci}^2}\frac{f}{\left[1+\frac{f^2}{f_{ci}^2}\right]^2} \quad (10)$$

The first derivative of each single Lorentzian has a minimum at the frequency $f_{ci}/\sqrt{3}$ that depends on the nature of the detected gas.We have demonstrated that the complete expression of the first derivative of the PSD of the gas sensor noise has a minimum at a frequency between $f_{c1}/\sqrt{3}$ and $f_{cg}/\sqrt{3}$ [25]. The extraction of this minimum thus enables to characterize the nature of the detected gas.

4.4 Product of the noise current spectral density by the frequency

Another gas identification method is based on the product $f\cdot\left(S_{\delta I_{sensor}}(f)-S_{Th}(f)\right)$ where *f* is the frequency, $S_{\delta I_{sensor}}(f)$ is the PSD of gas sensor noise current (9) and $S_{th}(f)=\frac{4kT}{R_{sensor}}$.

This product is written as follows:

$$f \cdot \left(S_{\delta I_{sensor}}(f) - S_{Th}(f)\right) = \frac{V_0^2}{R_{sensor}^4} \sum_{i=1}^{g} S_i \frac{f}{1 + \left(\frac{f}{f_{ci}}\right)^2} \quad (11)$$

The product of frequency by the PSD of the gas sensing layer resistance fluctuations often has a maximum which is characteristic of the gas and, that is the combination of maxima of each term [16]. The extraction of the maximum of the product also enables to characterize the nature of the gas detected.

5. Results

In this section, we first present the results of the extraction of the frequency attributes from the spectra measured under the three target gases. Then, the results of the PCA on the created database are given and discussed.

5.1 Spectral decomposition of the noise responses under different gases

The developed gas identification methods are based on precise spectral decomposition of measured noise responses. To extract useful information from the measured noise across the sensor in the presence of gas, we take into account the characteristics of low noise amplifier by:

$$S_{\delta I\,sensor} = \frac{S_{\delta V\,measured}}{\left(A_{LNA}(f)\right)^2} \quad (12)$$

where $S_{\delta I\,sensor}$ is the intrinsic current spectral density of sensor, and $S_{\delta V\,measured}$ is the measured noise voltage spectral density. $A_{LNA}(f)$ is the measured frequency response of

the gain of the SR570 low noise current amplifier. Fig. 4 gives an example of current spectral density of the sensor under 10ppm of CO (curve1).

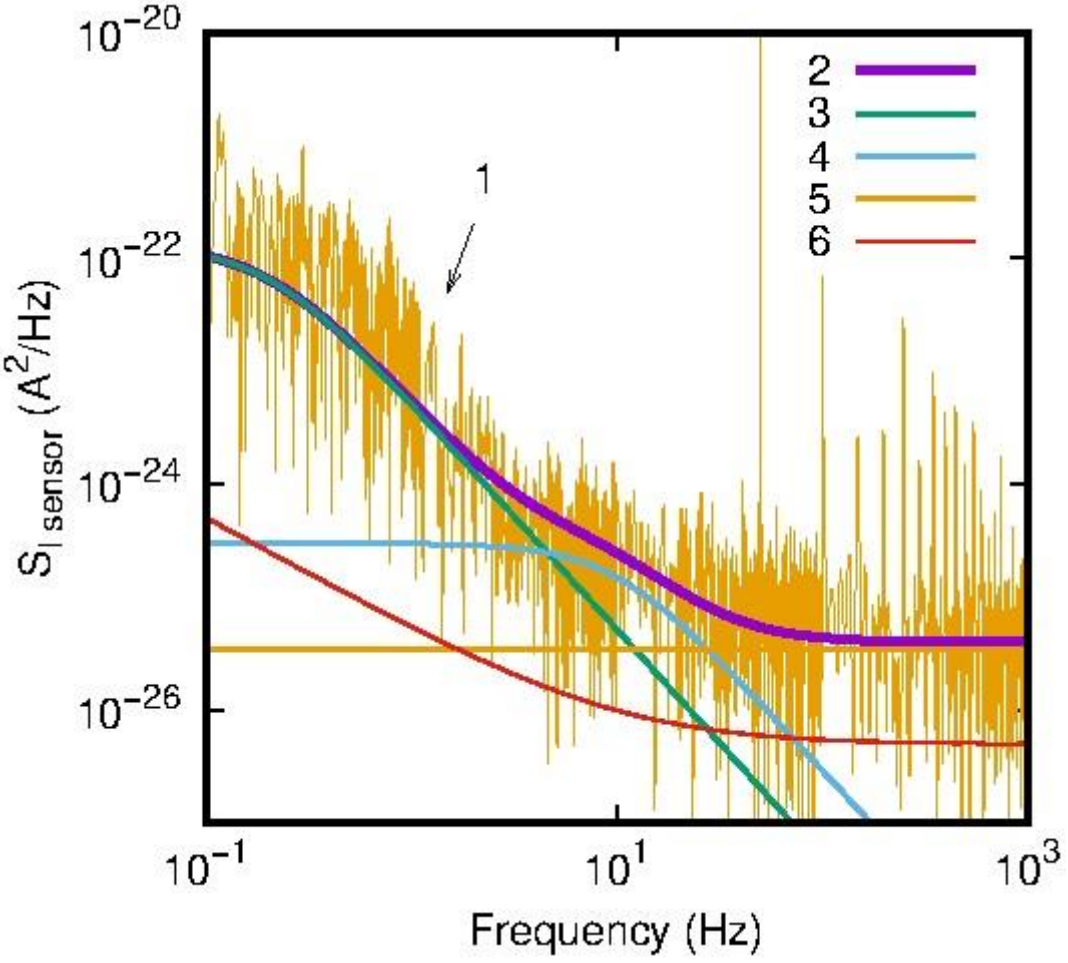

Fig. 4. Spectral decomposition of a noise response under CO (10 ppm): measurements (curve 1), total noise (curve 2), adsorption-desorption noise modeled by lorentzians (curve 3 and curve 4), white noise proportional to the resistance of the sensor (curve 5) and extracted noise model of low-noise current preamplifier (curve 6).

All measured spectra clearly show Lorentzian components according to adsorption-desorption noise theory. Indeed, the noise generated due to the adsorption of a gas on one type of adsorption site, with a given adsorption energy, has a Lorentzian spectrum. For the three studied gases, we observe that two Lorentzians dominate the low frequency spectrum. Over 1 kHz we observe white noise mainly composed of the thermal noise due to sensitive layer

resistance and the thermal noise of the amplifier due to the feedback resistor. Details of spectral decomposition are also plotted in Fig. 4. Measured noise spectra is higher by one or more orders of magnitude compared to amplifier noise level (curve 6). The extracted noise parameters of spectral decomposition of all measured spectra are reported in Table II, according to notations of equation (9). The values and the variation ranges of spectral parameters are specific for each gas. For all studied gas concentrations, the evolution of thermal noise is consistent with the evolution of the resistance of the sensitive layer in the presence of each of the three studied gases.

TABLE II. EXTRACTED NOISE PARAMETERS OF SPECTRAL DECOMPOSITION OF ALL MEASURED SPECTRA

Gas / Concentration	S_1 (A^2/Hz)	f_{C1} (Hz)	S_2 (A^2/Hz)	f_{C2} (Hz)	S_{Th} (A^2/Hz)
O_3 / C1	$7\ 10^{-21}$	0,1	$1\ 10^{-25}$	5	$3\ 10^{-26}$
O_3 / C2	$8\ 10^{-21}$	0,1	$1\ 10^{-25}$	5	$2,5\ 10^{-26}$
O_3 / C3	$1\ 10^{-20}$	0,1	$4\ 10^{-25}$	5	$2\ 10^{-26}$
O_3 / C4	$1,2\ 10^{-20}$	0,1	$5\ 10^{-25}$	5	$1,5\ 10^{-26}$
NO_2 / C1	$3\ 10^{-23}$	0,2	$7\ 10^{-25}$	5	$5\ 10^{-26}$
NO_2 / C2	$2\ 10^{-23}$	0,2	$9\ 10^{-25}$	5	$4,5\ 10^{-26}$
NO_2 / C3	$1,5\ 10^{-23}$	0,2	$7\ 10^{-25}$	5	$4\ 10^{-26}$
NO_2 / C4	$1\ 10^{-23}$	0,2	$7\ 10^{-25}$	5	$3,5\ 10^{-26}$
CO / C1	$1,2\ 10^{-22}$	0,2	$7\ 10^{-25}$	10	$2,5\ 10^{-26}$
CO / C2	$1,3\ 10^{-22}$	0,2	$3\ 10^{-25}$	10	$2,8\ 10^{-26}$
CO / C3	$1,5\ 10^{-22}$	0,2	$3\ 10^{-25}$	10	$3\ 10^{-26}$
CO / C4	$2\ 10^{-22}$	0,2	$3\ 10^{-25}$	10	$3,2\ 10^{-26}$

5.2 First derivative of the PSD of the noise responses under different gases

The first derivative of noise current spectral density of the measured gas sensor noise is calculated as (2) using extracted parameters of TABLE II. In Fig.5 we present the plots of the

first derivative of the PSD of the gas sensor noise response under four concentrations of nitrogen dioxide. We have similar curves for ozone and carbon monoxide. For the three gases, we clearly observe that the first derivative of the measured gas sensor noise spectrum presents a negative minimum at a frequency between $f_{c1}/\sqrt{3}$ and $f_{c2}/\sqrt{3}$, according to the developed theory in [26]. These negative minimums are reported in TABLE III and have specific value ranges for each gas. Such result shows the consistency of this gases identification method. The minimum of first derivative of PSD is rather sharp and depends on the nature of the detected gas.

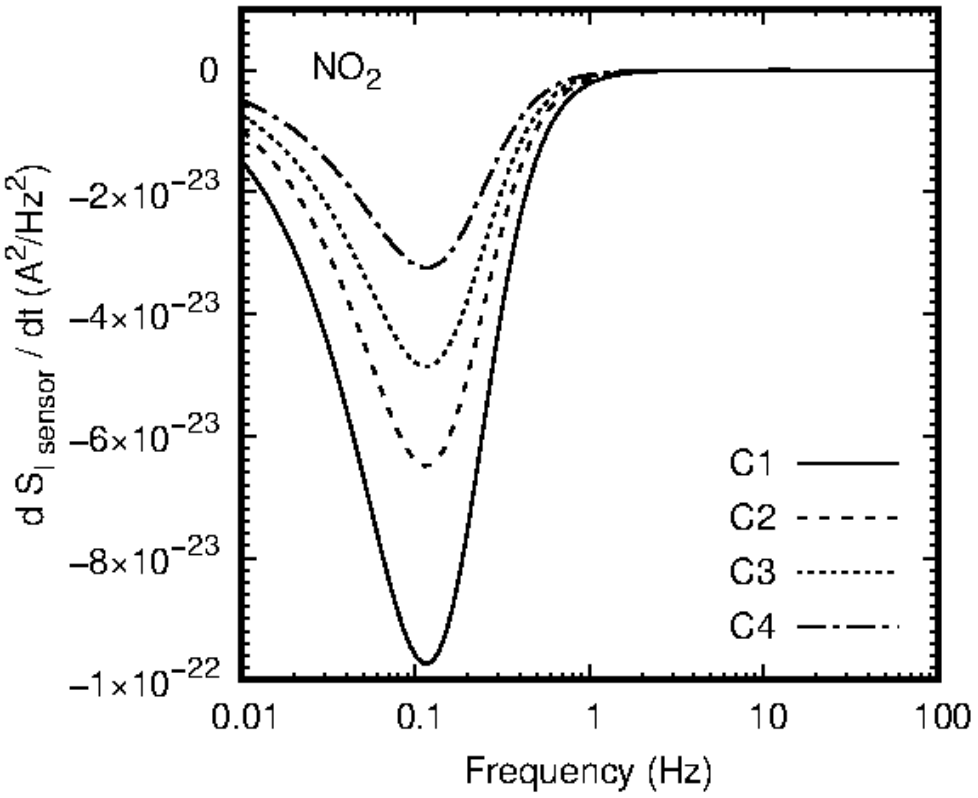

Fig. 5. Plots of the first derivtive of noise current spectral density for the four concentrations of nitrogen dioxide.

TABLE III. MINIMUM OF THE FIRST DERAVATIVE OF THE PSD OF NOISE CURRENT SPECTRAL DENSITY (A^2/Hz^2)

Gas	Concentration			
	C1	C2	C3	C4
O_3	$-4\ 10^{-20}$	$-5{,}2\ 10^{-20}$	$-6{,}2\ 10^{-20}$	$-7{,}8\ 10^{-20}$
NO_2	$-9{,}8\ 10^{-23}$	$-6{,}5\ 10^{-23}$	$-5\ 10^{-23}$	$-3{,}2\ 10^{-23}$
CO	$-3{,}9\ 10^{-22}$	$-4{,}2\ 10^{-22}$	$-4{,}9\ 10^{-22}$	$-6{,}5\ 10^{-22}$

5.3 Product of the PSD of the noise responses by the frequency

In Fig. 6, we plot the product $f \cdot \left(S_{\delta I_{sensor}}(f) - S_{Th}(f)\right)$ in the case of ozone, nitrogen dioxide and carbon monoxide using the extracted parameters in TABLE II. Over 100 Hz, we observe a 1/f slope as predicted in (11) for all concentrations of studied gases. On the other hand, at low frequencies, the behavior is different for each gas. For NO_2, the curves of the product of noise current spectral density by the frequency show two maximums of approximately equal values while the maximum at lower frequency is higher for CO. The curves for ozone have a particular behavior because of the higher sensitivity of tungsten trioxide to this gas. This high sensitivity to ozone is characterized by a higher low frequency noise level compared to other gases.

So, the quantity $f \cdot \left(S_{\delta I_{sensor}}(f) - S_{Th}(f)\right)$, has a maximum which is characteristic of the nature of the detected gas. Extracted maximums are reported in TABLE IV and have specific value ranges for each gas. Thus, detecting the maximum of the $f \cdot \left(S_{\delta I_{sensor}}(f) - S_{Th}(f)\right)$ is a sensitive method to identify a gas. This result confirms that the choice of this parameter seems interesting for the identification of the detected gas compared to other parameters such as the average slope of the product $f \cdot S_{\delta I_{sensor}}(f)$ [27] or the characteristic frequency of the maximum of this same product [28].

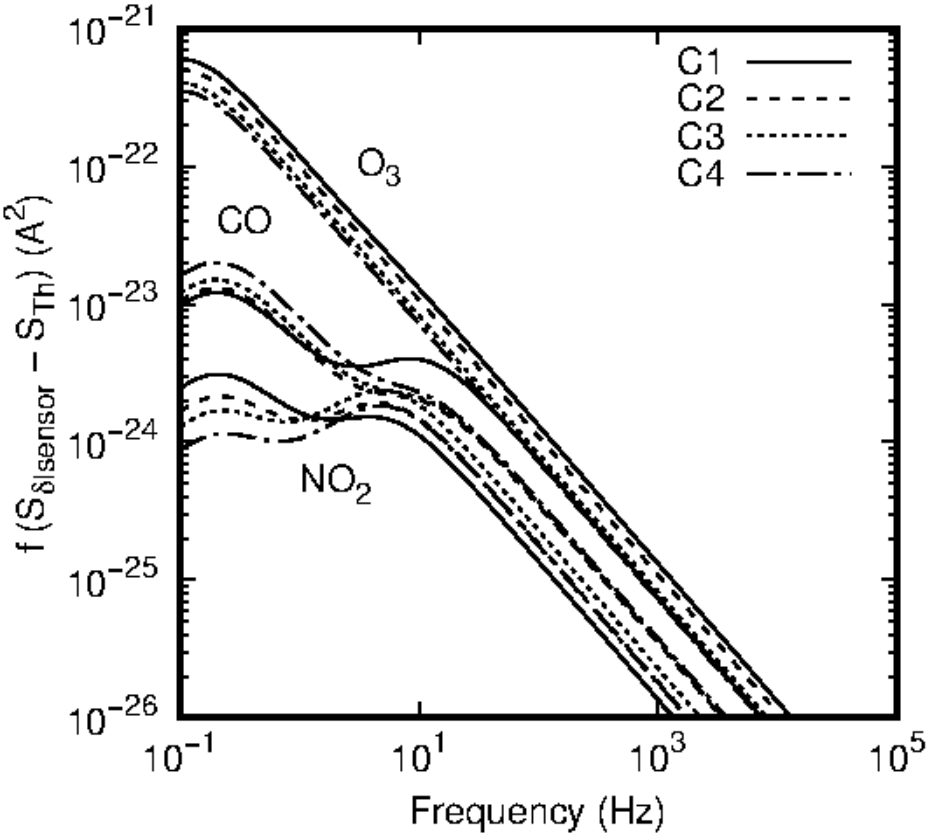

Fig. 6. Plots of the quantity $f \cdot \left(S_{\delta I_{sensor}}(f) - S_{Th}(f)\right)$ for four concentrations of ozone (O_3), nitrogen dioxide (NO_2) and carbon monoxide (CO) detected by metal-oxide gas microsensor with tungsten trioxide (WO_3) sensing layer.

TABLE IV. MAXIMUM OF THE PRODUCT OF THE PSD OF NOISE CURENT SPECTRAL DENSITY BY THE FREQUENCY (A^2)

Gas	Concentration			
	C1	C2	C3	C4
O_3	3,3 10^{-22}	4 10^{-22}	5 10^{-22}	6 10^{-22}
NO_2	3 10^{-24}	2 10^{-24}	1,3 10^{-24}	1,2 10^{-24}
CO	1,1 10^{-23}	1,2 10^{-23}	1,3 10^{-23}	2 10^{-23}

5.4 Data analysis for gas identification

For each of the three gas identification methods, we have shown that the extracted parameters were different for ozone, nitrogen dioxide and carbon monoxide. The ability to discriminate several gases using our different noise spectroscopy-based gas identifying

methods has been evaluated by the principal component analysis (PCA). Our noise database consists of Tables II, II and IV. The PCA enable us to convert the set of observation of correlated or uncorrelated variables of our database into a new set of values (principal components). Then, the score plots of PCA show the relations between these analyzed variables (different concentrations of the three gases in our studies). PCA has been performed using the Pearson matrix calculation. The PCA variables are the all extracted parameters of the spectral decomposition (TABLE II), the minimum of first derivative of noise current spectral density (TABLE III) and the maximum of the product of the PSD of noise current spectral density by the frequency (TABLE IV). The observations are the set of twelve concentrations of the studied gases.

The calculation of the correlation matrix shows that several variables are correlated and others uncorrelated. For our study, the first low frequency magnitude S_1 of spectral decomposition is correlated with the minimum of first derivative of PSD and the maximum of $f \cdot \left(S_{\delta I_{sensor}}(f) - S_{Th}(f)\right)$. Conversely, values of thermal noise are uncorrelated with values of cut-off frequency of the second lorentzian. About the variability of the PCA eigenvalues, the majority of the inertia is carried by two axes PC1 and PC2 (about 91% cumulated) which are therefore the two principal components. Table V presents the coordinates of the PCA variables according to PC1 and PC2. H_1 and Fc_1 are the low frequency magnitude and cut-off frequency of first lorentzian, respectively. H_2 and Fc_2 are the low frequency magnitude and cut-off frequency of second lorentzian, respectively. T_H is the thermal noise. Min_S_i' is the minimum of first derivative of PSD. F_0 is the frequency at this minimum and Max_fSi is the maximum of product of PSD by the frequency.

TABLE V. TABLE OF CORRELATIONS BETWEEN VARIABLES AND THE TWO PRINCIPAL COMPONENTS.

PCA Variable	PC1	PC2
H_1	0,992	-0,059
Fc_1	-0,988	0,051
H_2	-0,509	-0,578
Fc_2	-0,445	0,873
T_H	-0,720	-0,510
Min_S_i'	-0,988	0,051
F_0	-0,987	0,065
Max_fS_i	0,990	-0,049

All PCA variables have a significant length in the PC1 / PC2 plane. The PC1 axis is rather related to H_1 and Max_fS_i while the PC2 axis is rather related to the Fc_2 parameter. The scores plot of the first two principal components is given in Fig. 7. We clearly observe three groups of data. Each group corresponds to one gas. A first separation can be made according to the PC1 component. The corresponding ozone data has a strongly positive PC1 values due to a higher value of the H_1 and Max_fSi extracted parameters, while the NO_2 and the CO have negative PC1 values. The component PC2 makes it possible to separate these two gases. Indeed, the values for NO_2 have a negative value of PC2 and are therefore rather related to the parameter T_H and H_2. Conversely, the values for CO have a positive value of PC2. CO is further characterized by Fc_2 parameters. PCA results show that a clear discrimination is possible between the three studied gases.

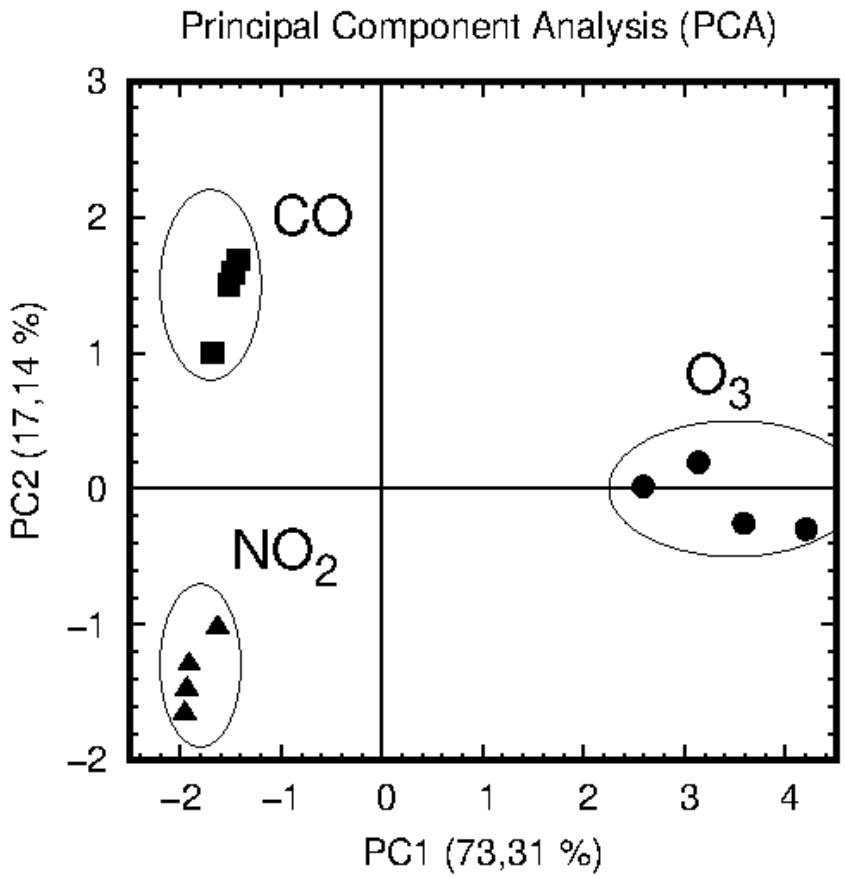

Fig. 7. PCA scores plot

These results were obtained with three gases diluted in dry air. Under actual conditions for measuring pollutants in the atmosphere, humidity is present in proportions ranging from 15% to almost 100%, and it is known that the response of MOX sensors is affected by the presence of humidity, which leads to a decrease of the sensor response. However, as explained in Section 2, noise spectroscopy provides a quantity of information greater by several orders of magnitude than that provided by a simple measurement of the resistance of the sensor. So, we may think that the spectral attributes studied in this article, associated with powerful classification algorithms such as Support Vector Machines, k Nearest Neighbors or Neural

Networks, will allow the identification of target gases to continue, even in the presence of humidity.

6. Conclusion

In this paper, we have presented new developments in gases identification methods using noise spectroscopy. These methods are based on precise spectral decomposition of measured noise responses of micro sensor under gases. For each method, we studied the ability to discriminate the nature of detected gas. In particular, the minimum of the first derivative of noise current spectral density is different for each studied gases. Similarly, we have observed that the maximum of the product of noise current spectral density by the frequency is characteristic of the nature of the detected gas. Finally, the PCA multivariable analysis method has been applied to all extracted spectral data and has shown that it is possible to identify the nature of three gas using noise spectroscopy-based methods applied to one single MOX gas sensor.

After these promising results, more work is in progress in order to:

- increase the database by adding more gases concentrations and mixing the gases with each other and with humidity;
- test the detection of other gases representative of air quality, such as BTEX (benzene, toluene, ethyl benzene, xylene);
- study whether the number of spectral attributes used for gases identification can be reduced;

- experiment classification algorithms such as Support Vector Machines, k Nearest Neighbors or Neural Networks.

Acknowledgement

Nicolas MORATI would like to thank Région Sud of France and Nanoz SAS for financial support.

References

[1] J. Gutiérrez, M.C.Horrillo, “Advances in artificial olfaction: sensors and applications”, Talanta 124, pp. 95–105, 2014

[2] L. Capelli , S. Sironi, R. Del Rosso, “Electronic Noses for Environmental Monitoring Applications”, Sensors 2014, 14, 19979-20007; doi:10.3390/s141119979

[3] J. Yan et al., « Electronic Nose Feature Extraction Methods: A Review », Sensors, vol. 15, n° 11, p. 27804-27831, nov. 2015.

[4] J. M. Smulko et al., “New approaches for improving selectivity and sensitivity of resistive gas sensors: a review”, Sensor Review, vol. 35, n° 4, p. 340-347, sept. 2015.

[5] L. B. Kish, R. Vajtai, and C.-G. Granqvist, “Extracting information from noise spectra of chemical sensors: Single sensor electronic noses and tongues”, Sens. Actuators B, Vol. 71, pp. 55–59, 2000.

[6] J. Solis, L. Kish, R. Vajtai, C. Granqvist, J. Olsson, J. Schnürer, and V. Lantto, “Identifying natural and artificial odours through noise analysis with a sampling-and-hold electronic nose”, Sensors and Actuators B: Chemical, Vol. 77, no. 1, pp. 312–315, 2001.

[7] T. Contaret, N. Morati, S. Gomri, T. Fiorido, J.-L. Seguin, M. Bendahan, “Noise spectroscopy-based gas identifying methods to improve the selectivity of MOX gas sensors”, 25th International Conference on Noise and Fluctuations (ICNF 2019), EPFL Neuchâtel campus - Neuchâtel, Switzerland, 18 - 21 June 2019. DOI: 10.5075/epfl-ICLAB-ICNF-269234.

[8] A. Ortega, S. Marco, A. Perera, T. Sundic, A. Pardo and J. Samitier, “An intelligent detector based on temperature modulation of a gas sensor with a digital signal processor”, Sens. Actuator B, 78(1-3) 32-39, 2001.

[9] T. Amamoto, T. Yamaguch, Y. Matsuura and Y. Kajiyama, “Development of pulse-drive semiconductor gas sensor”, Sensor. Actuators B, 14(1-3) 587-588, 1993.

[10] M. Pardo, L. G. Kwong, G. Sberveglieri, K. Brubaker, J. F. Scneider, W. R. Penrose and J.R. Stetter, “Data analysis for a hybrid sensor array”, Sensor. Actuators B, 106(1) 136-143, 2005.

[11] W. Göpel W and K. D. Schierbaum, “SnO2 sensors: current status and future prospects” Sensors Actuators B 26–27 1–12, 1999.

[12] M. A. Djeziri, S. Benmoussa, R. Sanshez. “Hybrid method for remaining useful life prediction in wind turbine systems”, Renewable Energy (2018). Renewable Energy. V. 116. pp. 173-187.

[13] L. Nguyen, M. A. Djeziri, B. Ananou, M. Ouladsine, J. Pinaton, “Fault prognosis for batch production based on percentile measure and gamma process: Application to semiconductor manufacturing” in Journal of Process Control, Vol.48. pp. 72-80 (2016).

[14] L. Nguyen, M. A. Djeziri, B. Ananou, M. Ouladsine, J. Pinaton, “Health Indicator Extraction for Fault Prognosis in Discrate Manufacturing Processes”, IEEE Transaction on Semiconductor Manufacturing, vol.28, no. 3, pp. 306-317, 2015.

[15] Hu, W., Wan, L., Jian, Y., Ren, C., Jin, K., Su, X., Bai, X., Haick, H., Yao, M., Wu, W., “Electronic Noses: From Advanced Materials to Sensors Aided with Data Processing”, Advanced Materials Technologies 4, 2019 1800488. https://doi.org/10.1002/admt.201800488.

[16] S. Gomri, J.L. Seguin, T. Contaret, T. Fiorido, K. Aguir, “A Noise Spectroscopy based Selective Gas Sensing with MOX Gas Sensors”, Fluctuation and Noise Letters., Vol.17, No.2, (2018).

[17] H. Wong, “Low-frequency noise study in electron devices: review and update”, Microelectron. Reliab. 43 585–99, 2003.

[18] F. N. Hooge, T. G. M. Kleinpcnning and L. K. J. Vandamme, Rep. Prog. Phys. 44, 479, 1981.

[19] A. L. McWhorter, Semiconductor Surface Physics (Edited by R. H. Kingston). Univ. of Pennsylvania Press, 1957.

[20] T. Contaret, K. Romanjek, T. Boutchacha, G. Ghibaudo and F. Boeuf, “Low frequency noise characterization and modeling in ultrathin oxide MOSFETs”, Solid State Electronics, vol. 50 p 63-68, 2006.

[21] A.K. Raychaudhuri, “Measurement of 1/f noise and its application in materials science”, Current Opinion in Solid State and Materials Science, 6 67-85, 2002.

[22] T. Contaret, S. Gomri, J-L. Seguin and K. Aguir, “Noise spectroscopy measurements in metallic oxide gas microsensors”, IEEE Sensors 2008, Digital Object Identifier 10.1109/ICSENS.2008.4716417, pp 200-203, 2008.

[23] T. Wolkenstein, “Electronic Processes on Semiconductor Surfaces During Chemisorption”, translated from Russian by E. M. Yankovskii and edited by R. Morrison (Consultants Bureau, New York), 1991.

[24] S. Gomri, J.L. Seguin, J. Guerin and K. Aguir, “A mobility and free carriers density fluctuations based model of adsorption-desorption noise gas sensor”, J. Phys.D: Appl. Phys. 41 065501 (11pp), 2008.

[25] S. Gomri, T. Contaret, J. Seguin, K. Aguir, M. Masmoudi, “Noise Modeling in MOX Gas Sensors”, Fluctuation and Noise Letters, Vol. 16, No. 2 (2017) 1750013.

[26] S. Gomri, T. Contaret, J. L. Seguin. "A New Gases Identifying Method with MOX Gas Sensors using Noise Spectroscopy", IEEE Sensors Journal, Vol.18, No.16, (2018) DOI: 10.1109/JSEN.2018.2850817.

[27] B. Ayhan, C. Kwan, J. Zhou, L.B. Kish, K.D. Benstein, P.H. Rogers, S. Semancik, “Fluctuation enhanced sensing (FES) with a nanostructured, semiconducting metal oxide film for gas detection and classification”, Sensors and Actuators B 188 (2013) 651-660.

[28] S. Rumyantsev, G. Liu, R. A. Potyrailo, A. Balandin, and Michael S. Shur, “Selective Sensing of Individual Gases Using Graphene Devices”, IEEE Sensors J. vol 13, NO. 8 (2013) 2818-2822.